LIMNOLOGY and OCEANOGRAPHY

ASLO

Limnol. Oceanogr. 67, 2022, 1402–1415

doi: 10.1002/lno.12091

Flexible habitat choice of pelagic bacteria increases system stability and energy flow through the microbial loop

Luis Alberto Villalba,[1] Rajat Karnatak,[1] Hans-Peter Grossart [1,2*] Sabine Wollrab [1*]
[1]Leibniz Institut of Freshwater Ecology and Inland Fisheries (IGB), Berlin, Germany
[2]University of Potsdam, Potsdam, Germany

Abstract

Pelagic bacteria can be classified into free-living and particle-attached life modes, which either dwell in the water column or attach to suspended particles. Bacteria with a generalist life style, however, can actively shift between these two habitats. Globally increasing densities of natural and artificial particles enhance habitat heterogeneity, with potential consequences for system stability and trophic transfer through aquatic food webs. To better decipher the dynamics of microbial communities, we investigated the influence of adaptive vs. fixed habitat choice on species coexistence for a simplified bacterial community by analyzing a corresponding food web model, consisting of two specialist bacterial prey species (free and attached), a generalist bacterial prey species with the ability to shift between both habitats, and two protist predators, specialized on either water or particle compartment. For simplicity we assume a shared resource pool, considering particles only for colonization but not as a source for nutrients or carbon, that is, inert particles like microplastics or inorganic sediments. The model predicts coexistence on a cyclic attractor between fixed and flexible bacteria, if the costs for adaptive habitat choice can be balanced by adaptation speed. The presence of adaptive prey dampens predator–prey cycle amplitudes, contributing to system stabilization resulting in higher mean predator biomass compared to specialist prey only. Thus, in pelagic microbial systems, flexible habitat choice at the prey level has important implications for system stability and magnitude of energy flow through the microbial loop.

Aquatic environments sustain highly diverse heterotrophic microbial communities which can rapidly change in space and time due to fluctuations in natural conditions. In pelagic environments, heterotrophic bacteria play an important role in the recycling of nutrients from organic matter such as dissolved organic carbon (DOC) or particulate algal detritus, rendering them available for new primary production (Williams and leB. 1981; Cho and Azam 1988; Pomeroy et al. 1991). At the same time, bacteria are under high grazing pressure by bacterivorous protists (Fenchel 1984; Hahn et al. 2000; Garcia-Chaves et al. 2015) and a substantial fraction of bacterial biomass is directly transferred toward higher trophic levels through grazing by protozoa, the so called "microbial loop" (Azam et al. 1983). The microbial loop can form an important alternative energy channel at the base of the aquatic food web. For example, in oligotrophic environments (e.g., open ocean waters) with low abundance of phytoplankton species or dominance of very small sized phytoplankton, which cannot effectively be grazed by metazoans, the main energy link to metazoans and thereby higher trophic levels is via phagotrophic flagellates and ciliates (Sherr and Sherr 1988). Thus, under certain circumstances bacteria and protist interactions in pelagic environments play a key role in order to sustain aquatic food webs.

Pelagic environments contain two main habitats for bacterial colonization and activity (Grossart 2010): (1) the water and (2) particles or aggregates suspended in the water. The source of particles in aquatic systems is highly diverse, ranging from abiotic inorganic material (e.g., sediments, calcite, minerals, etc.) to allochthonous organic debris (e.g., wood, carcasses, detritus, etc.) and autochthonous organic matter such as single phytoplankton cells or macroscopic organic aggregates, that is, "marine or lake snow" (Simon et al. 2002; Kiørboe et al. 2003). Although the density and source of particles naturally varies in aquatic environments, an increased frequency of extreme weather events due to current climate change, including heavy rainfalls, floods, and strong winds, will likely increase the input of suspended particles from the terrestrial to the aquatic environment (Perga et al. 2018). In addition, anthropogenic pollutants like microplastics have been shown to increase globally in oceans (Law 2017), freshwaters (Eerkes-Medrano et al. 2015), polar environments (Obbard

*Correspondence: hgrossart@igb-berlin.de; wollrab@igb-berlin.de

Additional Supporting Information may be found in the online version of this article.

Author Contribution Statement: Concept: LAV, HPG, SW; Model: LAV, RK, SW; Manuscript: LAV, RK, HPG, SW

et al. 2014), and even pristine mountain lakes (Free et al. 2014). These nutrient poor particles interfere with the dynamics of natural microbial communities as they serve as a new surface for microbial colonization, potentially changing development and role of free-living vs. particle-attached bacteria.

To some extent, related to habitat and resource utilization, two main specialized life modes can be distinguished among heterotrophic bacteria in the pelagic environment. (1) free-living bacteria (B_{FL}) with very efficient nutrient uptake and transporter systems that allow them to cope with low nutrient conditions in the ambient water (Garcia et al. 2013), and (2) particle-attached bacteria (B_{PA}) that are specialized in attaching to particles (Simon et al. 2002; Grossart 2010). In addition to these two lifestyle specialists, generalist bacteria (B_G) are able to dwell in both habitats, involving an active behavioral response for habitat choice, that is, particles or water (Seiler et al. 2017). Note that while in microbiology the definition of specialist vs. generalist is often related to resource use, in the context of our study system the definition of specialist vs. generalist refers solely to habitat choice. The ability to adapt allows generalist bacteria to actively shift between different micro-habitats mostly by being associated with the water–particle interface. Especially, the water–particle interface acts as a microbial hotspot and plays a key role for microbial activity, but also holds a remarkably high grazing pressure (Kiørboe et al. 2004; Corno et al. 2015). The ability to escape predation by actively shifting habitats enables generalist bacteria to optimize habitat choice with respect to predation pressure. Depending on their feeding behavior, phagotrophic protists are either specialized on grazing in the pelagic habitat or on surfaces (e.g., particles), that is, free-living or particle-attached bacteria, respectively. Although free-living protists mainly feed on suspended bacteria by filtering or direct interception using cilia (Ciliates, e.g., *Paramecium tetraurelia*), or by creating water currents with a flagellum towards their mouth (Flagellates: e.g., *Cafeteria roenbergensis*) (Boenigk and Arndt 2002), protists specialized on particles need to be attached to surfaces where they, supported by pseudopods (e.g., Ameboids like *Vannella* sp.), feed on particle-attached bacteria (Parry 2004).

A behavioral predator escape mechanism is one form of adaptive phenotypic plasticity (sensu Gaedke and Klauschies 2017). For unicellular bacteria this adaptive behavior is often associated with a more complex genotype which enables the species to rapidly respond to a wide range of environmental conditions, providing adaptive species an advantage especially under variable conditions (Kassen 2002). However, this flexibility comes at a cost, as maintenance of the sensory and regulatory machinery needed for plasticity results in increased metabolic costs (energy demand) compared to the habitat specialists (DeWitt et al. 1998). Specifically, bacterial habitat generalists need to be able to exhibit a wider variety of traits related to habitat use compared to the bacterial habitat specialists. They need motility in their free-living life mode via corresponding flagella, but also require the ability to find particles via chemotaxis, enabling bacteria to attach to and colonize surfaces in the particle-attached life mode. Furthermore, bacterial habitat generalists need to detect the presence of predators, often by the recognition of chemical cues (Kats and Dill 1998), to correspondingly adapt habitat choice. In the specific case of generalist bacteria in the pelagic habitat, the ability to escape high predation pressure in one habitat (i.e., water or particles) makes them vulnerable to predation in the alternative habitat, a situation that has been termed incompatible defense (Ellner and Becks 2011; van Velzen et al. 2018).

It is known that adaptive prey dynamics feedback to the predator and competitor level, leading to system dynamics that can significantly differ from the case of fixed traits. This has been demonstrated by theoretical (Abrams and Matsuda 1997; Vos et al. 2004) as well as empirical studies (Yoshida et al. 2003; Verschoor et al. 2004). For example, classic predator–prey cycles assuming species with fixed traits, typically show a quarter-period lag between prey and predator peaks (Rosenzweig and MacArthur 1963; Bulmer 1975). However, in the presence of inducible defense mechanisms at the prey level, similar to rapid evolution (Yoshida et al. 2003; Jones and Ellner 2007; Becks et al. 2012), predator–prey dynamics can shift to antiphase cycles where the peaks in prey population overlap with minima in the predator population and vice versa in theoretical studies (Mougi 2012*b*; Yamamichi et al. 2019*a*).

To investigate the interplay of adaptive and nonadaptive strategies in the context of particle-attached vs. free-living bacterial lifestyles, we investigated the dynamic features of a corresponding food web model dependent on nutrient availability, the energetic costs of being adaptive and the speed of adaptation. The food web consists of a free-living and a particle-attached specialist bacterium and their respective habitat-specialized protist predators, as well as a generalist bacterial prey with the ability to actively switch between the two habitats in order to maximize its own growth. Our modeling approach considers one shared resource pool for all prey species. Thus, particles in our model system are considered as a habitat but do not provide a source of carbon or nutrients. Correspondingly, model results are most representative for inert particles such as inorganic sediments and microplastics suspended in the water column, but may not be adequate for organic matter rich particles such as marine and lake snow which frequently occur in natural ecosystems (Simon et al. 2002).

Our results show that coexistence between specialist and generalist bacteria strongly depends on the interplay of associated costs and speed of adaptation, but also on nutrient availability in the surrounding water. Single predator–prey lags are significantly longer for the generalist in comparison to specialist prey species and range from shorter than a quarter-period to lags well above 0.5. The latter is indicative of reversed cycle dynamics where the prey peak seems to follow the predator peak, while in classic predator–prey cycles the predator peak typically follows the prey peak (Cortez and Weitz 2014). This can occur if population dynamics are regulated by internal trait shifts which determine the edibility to the predator. Observed total predator–prey lags are significantly larger than quarter-period, ranging from antiphase to reversed cycle dynamics. In contrast, the effective

prey biomass per compartment is always close to a quarter-period lag. Overall the presence of the generalist stabilizes system dynamics by pushing population minima away from zero and albeit its ability to escape predation, the presence of the generalist leads to higher average protist biomass compared to the case with only nonadaptive prey. This indicates that the presence of prey species with adaptable lifestyle in the pelagic microbial community has important consequences for the transfer of energy via the microbial loop to higher trophic levels, with important implications for energy flow in pelagic food webs.

Material and methods

Model description

Our model food web consists of three prey species and two predators (Fig. 1B). Based on the distinction between the two pelagic compartments (1) ambient water and (2) particles, the prey species consist of two specialist bacterial species: a (nonattached) free-living bacterium (B_{FL}) and a particle-attached bacterium (B_{PA}), as well as a generalist bacterial species (B_G) that can actively switch between both compartments. The two predators are either specialized to be free-living (P_{FL}) or particle-attached (P_{PA}). Accordingly, P_{FL} only feeds on B_{FL} and the part of the generalist population in the water compartment, while P_{PA} only feeds on B_{PA} and the part of the generalist population in the particle compartment. The limiting substrate is assumed to be carbon and follows chemostat dynamics with maximum substrate concentration S_{max} (mg C L^{-1}) and dilution rate D (d^{-1}) (Eq. 1). All bacteria are assumed to share the same carbon pool, that is, particles themselves are not a source of carbon, therefore our system can be assumed to be representative for inorganic particles, but may not be adequate for organic matter rich particles. Bacterial prey and protist predator biomasses are expressed in carbon content (mg C L^{-1}). The corresponding ordinary differential equation (ODE) system (Eqs. 1–7) is based on a model system introduced by Gaedke and Klauschies (2017) on incompatible defense mechanisms via adaptive phenotypic plasticity such as adaptive behavior.

$$\frac{dS}{dt} = D \times (S_{max} - S) - \left(\left(\frac{r \times B_{FL} \times S}{H+S}\right) + \left(\frac{r \times B_{PA} \times S}{H+S}\right) + \left(\frac{r \times (1-c) \times B_G \times S}{H+S}\right)\right), \quad (1)$$

$$\frac{dB_{FL}}{dt} = \left(e_B \times \left(\frac{r \times S}{H+S}\right) - D\right) \times B_{FL} - g \times \left(\frac{B_{FL}}{B_{FL} + (1-\alpha)^n \times B_G + K}\right) \times P_{FL}, \quad (2)$$

$$\frac{dB_{PA}}{dt} = \left(e_B \times \left(\frac{r \times S}{H+S}\right) - D\right) \times B_{PA} - g \times \left(\frac{B_{PA}}{B_{PA} + \alpha^n \times B_G + K}\right) \times P_{PA}, \quad (3)$$

$$\frac{dB_G}{dt} = \left(e_B \times \left(\frac{r \times (1-c) \times S}{H+S}\right) - D\right) \times B_G - g \times \left(\frac{(1-\alpha)^n \times B_G}{B_{FL} + (1-\alpha)^n \times B_G + K}\right) \times P_{FL} - g \times \left(\frac{\alpha^n \times B_G}{B_{PA} + \alpha^n \times B_G + K}\right) \times P_{PA}, \quad (4)$$

$$\frac{dP_{FL}}{dt} = \left(e_P \times g \times \left(\frac{B_{FL} + (1-\alpha)^n \times B_G}{B_{FL} + (1-\alpha)^n \times B_G + K}\right) - D\right) \times P_{FL}, \quad (5)$$

$$\frac{dP_{PA}}{dt} = \left(e_P \times g \times \left(\frac{B_{PA} + (\alpha)^n \times B_G}{B_{PA} + (\alpha)^n \times B_G + K}\right) - D\right) \times P_{PA}, \quad (6)$$

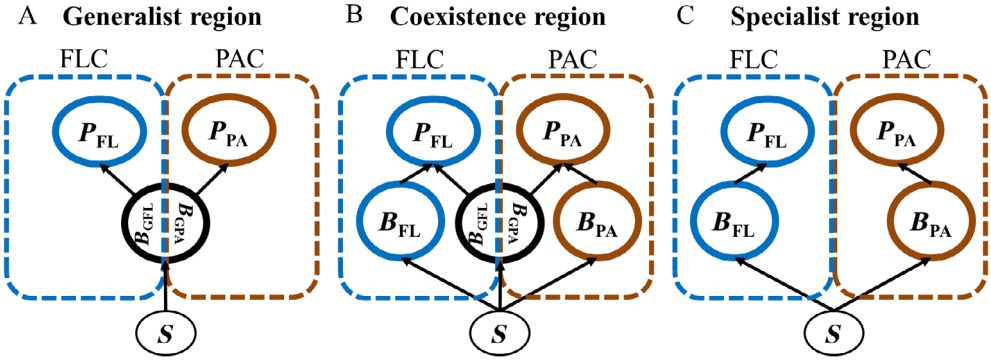

Fig. 1. Alternative possible system states dependent on the energetic cost and speed of adaptation. (**A**) Generalist region, (**B**) coexistence region, (**C**) specialist region. Illustrated are the free-living compartment (FLC) in blue and the particle-attached compartment (PAC) in brown. Specialist prey bacteria and predators are encircled in respective colors. The generalist (thick black circle) can shift between both habitats, indicated by different labels for the two subpopulations (B_{GFL} and B_{GPA}). *S* illustrates the shared carbon pool.

$$\frac{d\alpha}{dt} = V \times \left(\frac{\partial \left(\frac{1}{B_G} \frac{dB_G}{dt} \right)}{\partial \alpha} \right) + \frac{w}{\alpha^2} - \frac{w}{(1-\alpha)^2}. \quad (7)$$

The food uptake term of bacterial prey and protist predators follows a saturating functional response with maximum growth rate r and half saturation constant H for prey (Eqs. 2–4) and with grazing rate g and half saturation constant K for predators (Eqs. 5–6). Consumed resource/prey is converted into own biomass with conversion efficiencies e_B and e_P for bacteria and predators, respectively. For simplicity and to focus on the effect of the adaptability of the generalist, all nutrient/food uptake parameters are assumed to be identical for all prey/predator species, respectively (see Table 1). Investigations on the influence of a nonidentical parameterization and assumptions of different assimilation efficiencies for prey vs. predators can be found in the supplemental material (*see* Supporting Information S1 and S2). The growth rate r of the generalist prey species is reduced by a factor c, which represents energetic costs associated with its ability to adapt (Eq. 4).

The adaptive trait parameter α indicates the rate of attachment and can vary between 0 and 1. Thereby, α indicates the fraction of the generalist population that is in the particle-attached compartment given by $B_{GPA} = B_G \times \alpha$, while $(1-\alpha)$ indicates the fraction of the generalist population in the free-living compartment given by $B_{GFL} = B_G \times (1-\alpha)$. Each predator can consume the subpopulation of the generalist B_G (B_{GFL} and B_{GPA}) in its respective compartment as determined by α. In our study system, the trait parameter "rate of attachment" α defines a behavioral response and changes to increase the per-capita population growth rate of the generalist along the fitness gradient (Abrams et al. 1993; Yamamichi et al. 2019*a*). It has been argued by Abrams et al. (1993) and recently reviewed by Yamamichi et al. (2019*a*), that inducible defense mechanisms, due to the fact that they may even be faster than evolutionary changes, can be described by a fitness gradient approach, which typically is used for the description of the evolution of quantitative traits, if modified to allow for greater speed of adaptation. The trait value thereby represents the population mean of a continuous defense trait (in our case habitat choice). Different to an optimal adaptive trait approach which assumes an instantaneous response without any time delay, the fitness gradient approach allows to investigate the influence of different speeds of adaptation on system dynamics (Yamamichi et al. 2019*a*). Thereby the fitness gradient approach allows to gain insight on how species-specific differences in the speed of adaptation influence system dynamics. Consequently, we describe the trait dynamics of the rate of attachment (α) by a fitness function (Eq. 7), where a change in trait α depends on the change in net-growth of the generalist population (B_G) with a change in α, expressed by a corresponding partial derivative, multiplied by the speed of adaptation (V). This first part of Eq. 7 is followed by a boundary function $\left(\frac{w}{\alpha^2} - \frac{w}{(1-\alpha)^2}\right)$ which keeps α within the interval of [0; 1] (Yamamichi et al. 2019*a*). The shape parameter n (Eqs. 4–6) influences the shape of the trade-off between the susceptibility of B_G against predation by P_{PA} and P_{FL}. For $n = 1$ this trade-off is assumed to be linear. For values below 1, per-capita predation pressure on B_G is increased for intermediate values of α compared to the linear case, correspondingly the generalist experiences a higher predation pressure in comparison to the specialist prey species. Thereby our choice of $n = 0.8$ accounts for an additional cost for the generalist in comparison to the specialist prey species, termed "ecological cost" by Gaedke and Klauschies (2017). Note that with $n = 0.8$ the increase in predation pressure in comparison to the specialist prey species is small. Therefore, the assumption of a

Table 1. Parameter values, units, and description.

Parameter	Value	Unit	Description
D	0.1*	d^{-1}	Dilution rate
S_{max}	0.5 and 1	mg C L^{-1}	Maximum substrate concentration
r	3.33*	d^{-1}	Maximum growth rate of bacterial prey
c	[0;1]	—	Energetic cost
H	0.01*	mg C L^{-1}	Half saturation constant for substrate uptake
g	1.2*	d^{-1}	Maximum grazing rate of protist predators
n	0.8*	—	Shape of the trade-off between the susceptibilities to grazing by P_{FL} and P_{PA}
K	0.1*	mg C L^{-1}	Half saturation constant for prey ingestion
e_B	0.3*		Conversion efficiency for bacteria
e_P	0.3*		Conversion efficiency for predators
V	[0.01;1]	—	Speed of adaptation
w	0.0001*	d^{-1}	Scaling factor of boundary function

*Parameter values taken from Gaedke and Klauschies (2017).

linear trade-off ($n = 1$), that is, no additional costs, would benefit the generalist, slightly increasing the parameter range (c, V) where B_G is present (*see* Supporting Information S3).

Model analysis

We investigated the effect of flexible habitat choice of the generalist population B_G under top-down (predation) and bottom-up (resource competition) control on species coexistence and community dynamics. Note that coexistence in our study system and parameter values is only possible as part of an oscillatory attractor, since for a stable point equilibrium, the generalist prey species, due to the associated costs of being flexible, would always be outcompeted by the specialist prey species. To enable mechanistic insight on how the presence of the generalist species influences the system dynamics and how this depends on specific parameter values associated with the ability of a behavioral habitat choice, we restricted our analysis to levels of S_{max} where system dynamics equilibrate to regular limit cycle dynamics. The used parameterization is assumed to be representative for a bacterial prey-protist predator system following Gaedke and Klauschies (2017), but does not mimic a specific bacteria-protist system. All parameter values and investigated parameter ranges can be found in Table 1.

Possible community states and corresponding dynamics were investigated dependent on two parameters that are critical for the characterization of the adaptive life mode, namely the energetic cost of being adaptive c and the speed of adaptation V. We investigated the system dynamics by calculating the time orbits along transects of c (between 0 and 1) for fixed values of V and along transects of V (between 0.01 and 1) for fixed values of c. Starting at $c = 0$ ($V = 0.01$) system dynamics were followed for 5000 time units. The values from the last time point were used as starting condition for the next simulation run with slightly increased c-value (V-value) along each transect, increasing the respective parameter by a step size of 0.001. In addition, all transects have also been calculated in reverse direction, starting from the highest to the lowest c (V) value to look for possible hysteresis areas with bi-stability of alternative system states. The default initial condition at the starting point of each transect was ($S = 0.2$; $B_{FL} = 0.11$; $B_{PA} = 0.1$; $B_G = 0.11$; $P_{FL} = 0.01$; $P_{PA} = 0.01$; $\alpha = 0.5$). The slight difference in initial prey biomasses are chosen to avoid observed symmetry-driven pathological dynamics exhibited by the system—*see* Supporting Information S4 for details. For each simulation, maxima, minima, and average biomass per population cycle was calculated for each species based on the last third of the time orbit to avoid any influence of transient dynamics. Extinction of a given species was assumed if maximum biomass in the last third of the simulated time steps was bellow 10^{-5} mg C L^{-1}. For each simulation, after increasing V or c, a value of 0.0001 was added to the initial conditions of all species to allow for reinvasion in case of extinction in the previous simulation.

To assess the role of initial conditions and the stability of the observed attractors in our system, we recomputed the bifurcation diagram and the largest two Lyapunov exponents using random initial conditions. Find details on this analysis in Supporting Information S5.

To calculate the time lag between peaks of prey and predator pairs, we used the solution after the system has settled on regular dynamics (post-transient phase). Taking the last third of the calculated time points into account, we identified the consecutive cycle maxima of all species. The full cycle length was determined by the distance between two specialist predator peaks. Since for the standard parameterization cycle dynamics are exactly mirrored between compartments, the cycle length was estimated based on two consecutive maxima of the particle-attached predator (P_{PA}). Lag estimates were then calculated based on the peak distance between each prey and predator pair within two consecutive P_{PA} peaks divided by the full cycle length. For the generalist prey population predator–prey peaks were derived with respect to each predator, based on the distance between the peak of the generalist subpopulation and predator peak in the same habitat (defined by α). Since the total generalist population fluctuates two times faster compared to the specialist predator and prey populations, predator–prey lags for the generalist population were calculated based on (1) the full cycle length (of the generalist subpopulations/the specialist populations) (see Fig. 3, cycle length indicated in blue) as well as (2) the shorter cycle length of the total generalist population (see Fig. 3, cycle length indicated in black). Predator–prey lags were also calculated with respect to total predator-total prey biomass peaks (*see* Fig. 3, horizontal magenta arrows) and with respect to predator-effective prey peaks (*see* Fig. 3, horizontal green arrows). Effective prey biomass represents the prey biomass available to predation by the respective specialist predator (van Velzen and Gaedke 2017). In the generalist region, effective prey biomass is represented by the subpopulation of the generalist in each habitat available to the respective predator, in the coexistence region effective prey biomass is the sum of the generalist subpopulation and the specialist prey per habitat, and in the specialist region effective prey biomass equals the biomass of the specialist prey population for each habitat. A total of 10 consecutive cycle intervals were used to calculate the lag of each predator–prey pair (*see* examples for some cycle intervals and corresponding peaks in Supporting Information S6, Fig. S6.1).

Simulation of the system dynamics, time lag calculations, and bifurcation plots were performed using MATLAB (MathWorks R2018b) with Runge–Kutta solver ode45. Bifurcation plot and Lyapunov exponent calculations in Supporting Information S5 were done with Fortran using the double precision VODE ODE solver (Brown et al. 1989) to simulate the differential equation system. Fortran codes, along with VODE solver, can be found at https://github.com/legol18/Bifurcation-Lag-Lyapunov.

Results

Range of coexistence between specialists and generalist prey

The analysis of system states dependent on energetic costs for adaptation (c) and speed of adaptation (V) reveals three different regions (Fig. 2), (1) a *specialist region* where B_G is absent and only specialized prey (B_{FL} and B_{PA}) and predators (P_{FL} and P_{PA}) are present, (2) a *coexistence region* where all prey species and predators are present, and (3) a *generalist region*, where the two specialized prey species are out-competed by B_G and both predators exist on the generalist prey. The coexistence region extends to higher c values with increasing V, indicating that higher speed of adaptation allows the generalist to compensate for higher energetic costs and, therefore, to coexist with the specialist prey and predators. However, there seems to be an upper threshold of energetic costs close to 0.5, which is asymptotically reached for increasing values of V, above which a further increase in V cannot compensate for even higher energetic costs. Above this threshold, the generalist cannot persist and only specialists remain in the system. On the contrary, at low energetic costs and a high speed of adaptation, the generalist out-competes the two specialist prey species. The range of coexistence and generalist region increases with increasing nutrient availability (S_{max}) (compare Fig. 2A,B). Note that for $S_{max} = 0.5$, there is a small region with bi-stability at the intersection of specialist and coexistence region. It is increasingly pronounced for higher V-values as indicated by the thickness of the boundary line (Fig. 2B). In this area, initial conditions determine which of the two possible states will be reached.

Dynamics for different community states

For the investigated range of nutrient availabilities, dynamics of all community states settle on a limit cycle.

In the *generalist region* (Fig. 3A–D), B_G is fluctuating regularly between the free-living and particle-attached compartment, thereby maintaining both specialist predators. If B_G is dominantly in one compartment (α close to zero or one), the corresponding predator biomass increases over time. When predator biomass and therefore top down pressure on its prey is getting too high, B_G shifts quite abruptly to the alternative compartment, as indicated by the trait parameter α (Fig. 3D). Note that total B_G biomass cycles twice as fast as the single predator biomass of each compartment (comparing Fig. 3A,C), every second generalist peak corresponding to a specific compartment (Fig. 3D). The lag between peaks of the total generalist population per compartment and the peak of the respective specialist predator is significantly longer than the quarter-period lag period of classical predator–prey cycles, following values close to 0.3 (Fig. 4, gray line) and equals the effective predator–prey lags (Fig. 4, green line). When considering the shorter cycle length of the total B_G population instead of the longer cycle length of the B_G subpopulations (the specialist populations), the lag between the peak of total B_G biomass and the peak of the respective predator (indicated by the corresponding α value) is slightly longer than half-period following values close to 0.6 (Fig. 4, black line) and equals the total predator-total prey lags (Fig. 4, magenta line). In the *coexistence region* (Fig. 3E–H), the generalist population shows similar dynamics as in the generalist region, with B_G fluctuating two times faster compared to the two specialist predators and preys. For the specialist prey species, the lag of the predator–prey cycles within each compartment first slightly decreases with increasing c, starting from values close to a quarter-period lag (Fig. 4, brown line), while the predator–prey lags between B_G and the predator species remain close to the lag values of the generalist only case (Fig. 4, gray and black lines). This pattern changes around $c = 0.25$, beyond which all single predator–prey lags start to increase steeply, being most

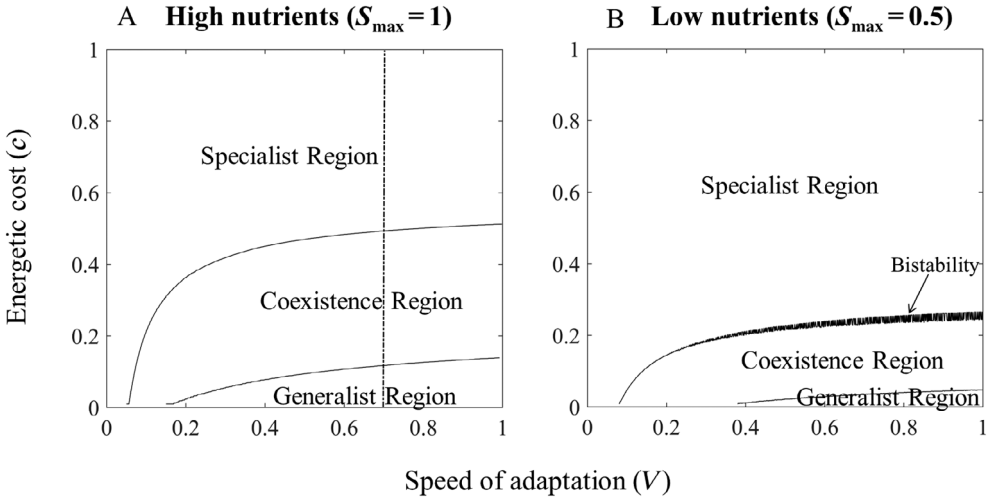

Fig. 2. Diagrams show different community states dependent on speed of adaptation V and energetic cost c for different nutrient availabilities: (**A**) $S_{max} = 1$, (**B**) $S_{max} = 0.5$. In (**B**), thickness of boundary between specialist and coexistence area indicates the extension of a bistability area. The vertical dashed line at $V = 0.7$ in (**A**) indicates the transect along c which was used for further analysis of cycle dynamics and predator–prey lags (Figs. 3–6).

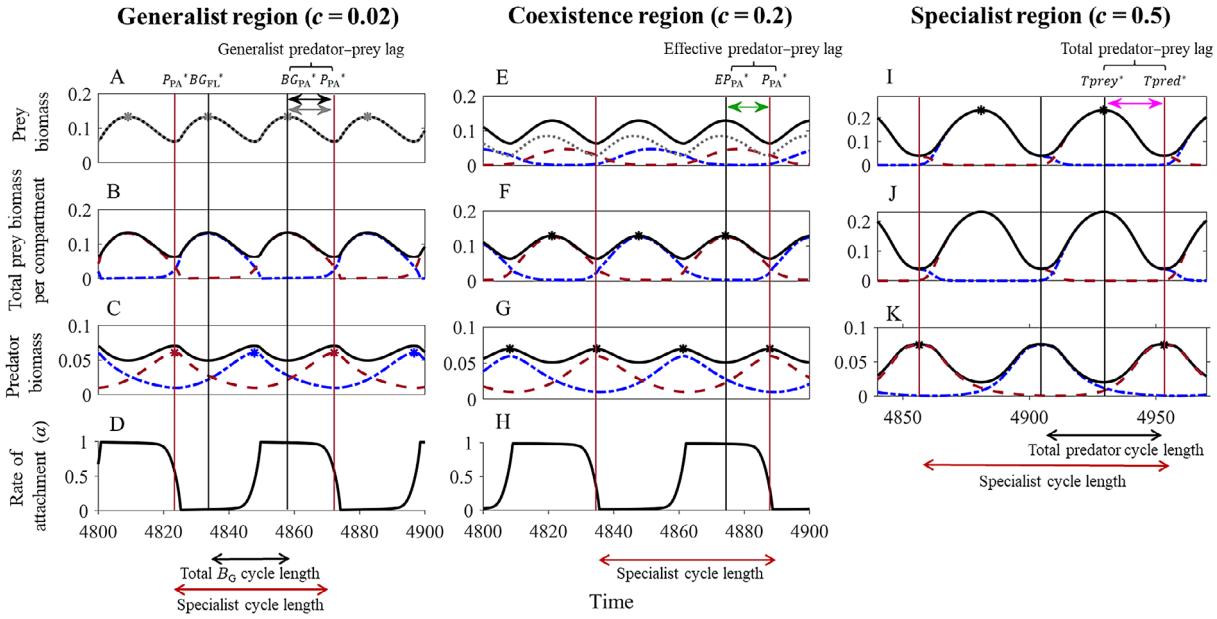

Fig. 3. Time orbits illustrating regular cycle dynamics for: Left column: Generalist region ($c = 0.02$), central column: coexistence region ($c = 0.2$), and right column: specialist region ($c = 0.5$). All scenarios are calculated for $S_{max} = 1$ and $V = 0.7$. Biomass units are expressed in mg C L^{-1}. In the upper three rows, black solid lines indicate total prey/predator biomass, dash-dotted blue (dashed brown) lines indicate prey/predator biomass of free-living (particle-attached) compartment. Note that in (**B**,**F**,**J**), total prey biomass per compartment is illustrated, whereas in (**E**,**I**) colored lines refer to individual populations. In (**E**), dash-dotted blue, dashed brown and dotted gray lines represent free-living, particle-attached specialist and generalist biomass, respectively. Colored horizontal arrows in (**A**,**E**,**I**) illustrate the lag between predator and prey peaks, the colors correspond to the respective lags plotted in Fig. 4: (**A**) generalist predator–prey lag (black, gray), (**E**) effective predator–prey lag (green) and (**I**) total predator–prey lag (magenta). Colored horizontal arrows in (**D**,**H**,**K**) illustrate: (**D**) the full specialist (brown) and shorter cycle length of B_G (black), defined by two consecutive peaks of P_{PA} and B_G, respectively, (**H**) the full specialist cycle length (brown), and (**K**) the total predator cycle length (black) defined by two consecutive peaks of total predator biomass. Note that due to the increase of the cycle's frequency the time interval on the *x*-axis differs between regions.

pronounced for the total B_G—predator lags with respect to the shorter B_G cycle length (Fig. 4, black line), which reach values of almost 0.8 at the extinction threshold of B_G ($c = 0.5$). The latter is indicative of reversed cycles; however, this is only true if total predator and total generalist prey peaks are taken into account irrespective of the generalists' habitat use. Taking habitat use into account, within each compartment the B_G prey peak still precedes the peak of its respective predator, the distance between the two increasing with increasing c. The lags of the specialist predator–prey pairs reach the typical quarter-period lag period at the extinction threshold of B_G, on which they settle constantly within the specialist region. The turning point at $c \approx 0.25$, where the lags start increasing, coincides with the change in dominance from the generalist to the specialist preys, indicated by a corresponding shift from $\max(B_G) > \max(B_{FL})$ for $c < 0.25$ to $\max(B_G) < \max(B_{FL})$ for $c > 0.25$ (and equally with respect to $\max(B_{PA})$; *see* Supporting Information S6, Fig. S6.2). In contrast to the single predator–prey lags, total predator–prey lags and predator-effective prey lags decrease steeply for $c < 0.25$, but settle on values close to the lags observed for the specialist region for values of $c > 0.25$. In the *specialist region* (Fig. 3I–L), population dynamics in each compartment are characterized by predator–prey cycles with fixed traits, where a prey peak is followed by a predator peak with a quarter-period lag (Fig. 4, brown line), while total predator–prey lags follow an antiphase cycle (Fig. 4, magenta line). The specialist food web and its dynamics can also be interpreted as a coevolution model with clonal reproduction (Mendelian/discrete trait) at the prey and predator level under a matching allele interaction (Grosberg and Hart 2000), which has been shown to be analogous to the bidirectional axis of vulnerability in quantitative (continuous) traits, the latter reflecting the generalist-two predator food web (Yamamichi et al. 2019*b*). Our findings of antiphase cycles for total predator–prey dynamics even for the specialist food web are therefore in concordance with previous studies showing that coevolution along a bidirectional axis of vulnerability can produce antiphase cycles (Mougi 2012*a*). Specifically, the decrease of a prey population in one compartment allows the prey species of the alternative compartment to increase, due to low competition for the shared resource in combination with low predator densities. This increase starts the predator–prey cycle in the respective compartment until, at low prey densities (after the predator peak), the cycle is reinitiated in the other compartment.

Shifts in timing of B_G peak with increasing energetic costs

In the coexistence region, we observe a continuation of the generalist-predator lags from the generalist only case for $c < 0.25$ and a pronounced increase in the generalist-predator

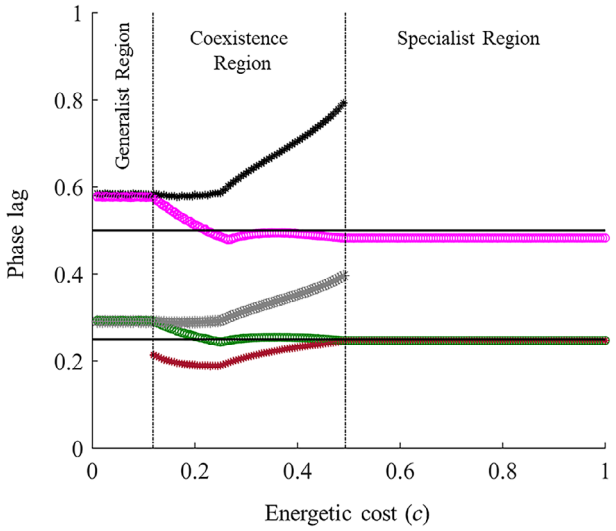

Fig. 4. Shifts in predator–prey phase lags with increasing energetic costs for: (i) the total generalist population B_G with respect to both predators P_{FL} and P_{PA}, the lag estimated based on the shorter cycle period of the generalist population (black line); (ii) the generalist subpopulations B_{GFL} and B_{GPA}, with respect to their respective predators P_{FL} and P_{PA}, the lag estimated based on the longer cycle period of the predators (generalist subpopulations) (gray line); (iii) the specialist species (B_{FL} and B_{PA}) with respect to their specialist predator (P_{FL} and P_{PA}) (brown line); (iv) the total prey to total predator lag (magenta line); and (v) the effective prey to predator lag per compartment (green line). Note that effective and single species to predator lags are identical between compartments, therefore for each case only one line is represented for the respective lags in both compartments. The horizontal solid black line represents the typical quarter-period and half-period lag. Calculation was carried out for $S_{max} = 1$ mg C L^{-1} and $V = 0.7$.

lags for $c > 0.25$ (Fig. 4, black and gray lines). Taking a detailed look at the cyclic dynamics for different values of c, we find that with increasing c, the timing of the generalist peak appears earlier after its shift to a compartment, indicated by α (Fig. 5). Looking at the maximum and total biomass, we observe that for $c = 0.2$ (Fig. 5A–C), B_G biomass is higher than the corresponding specialist prey biomass almost throughout the cycle (Fig. 5A). For $c = 0.3$ (Fig. 5D–F), the generalist dominates total prey population only until it peaks, for the rest of the cycle the specialist prey dominates the prey population in the respective compartment. At this value the specialist prey also reaches higher maximum values compared to the generalist (Fig. 5D). This indicates that with increasing c, predator biomass is more and more determined by the availability of the specialist prey. Therefore, the phase of the predator–prey cycle, determined by total available prey per compartment, extends compared to the generalist only case. For $c = 0.4$ this is even more pronounced (Fig. 5G–I). The generalist dominates the prey population only at a small time interval at the beginning of the cycle, and peaks at a much lower value compared to lower c values. Now, for most of the cycle, prey population is dominated by the specialist prey, and cycle length as well as the lag between generalist and predator peak is prolonged.

Accordingly, the timing of a complete shift of the generalist population from the free-living to the particle-attached compartment indicated by α shifting from one to zero (Fig. 5C,F,I), coincides with the predator peak in the free-living compartment for $c = 0.2$, but moves more and more to time points before the predator peak for higher c values (Fig. 5, indicated by vertical dashed brown line).

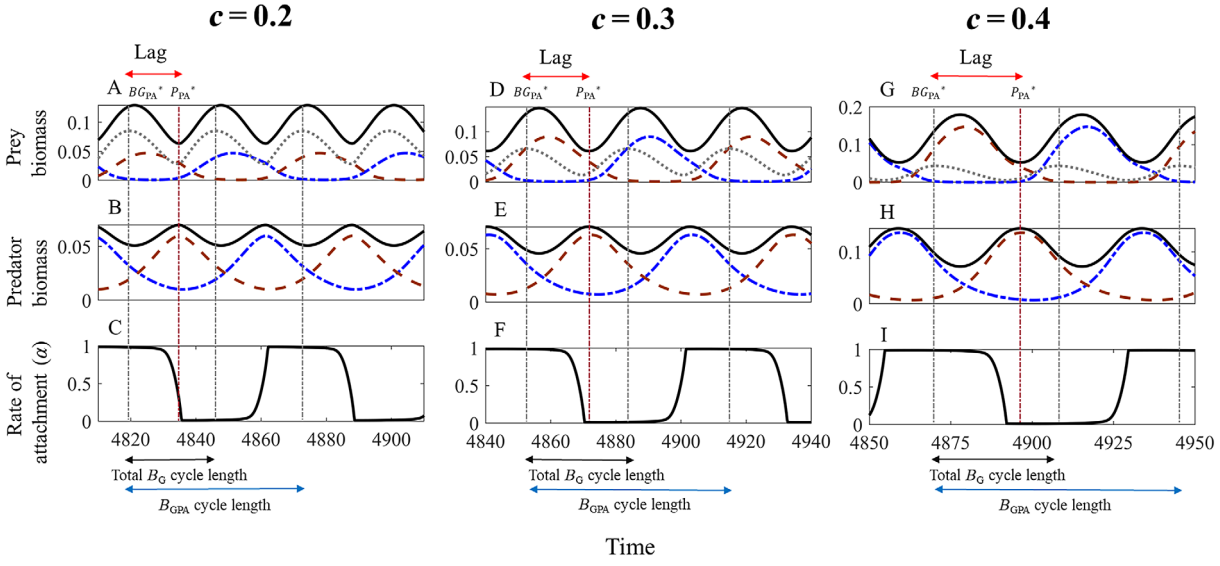

Fig. 5. Time orbits in the coexistence region for three different c values (0.2, 0.3, and 0.4). In the upper two rows, black solid lines indicate total prey/predator biomass, lines indicate generalist (gray dotted), free-living bacteria and predator (blue dashed), and particle-attached bacteria and predator (brown dashed). For each scenario, the timing of the first B_G maximum in the particle-attached compartment is indicated by a gray vertical dashed line and the timing of the corresponding predator peak P_{PA} by a dashed vertical brown line. Black and blue horizontal arrows (**C**,**F**) indicate the cycle length of total B_G population vs. the cycle length of the subpopulations, here illustrated for B_{GPA}. Biomass units are expressed in mg C L^{-1}. All graphs are calculated for $S_{max} = 1$ mg C L^{-1} and $V = 0.7$.

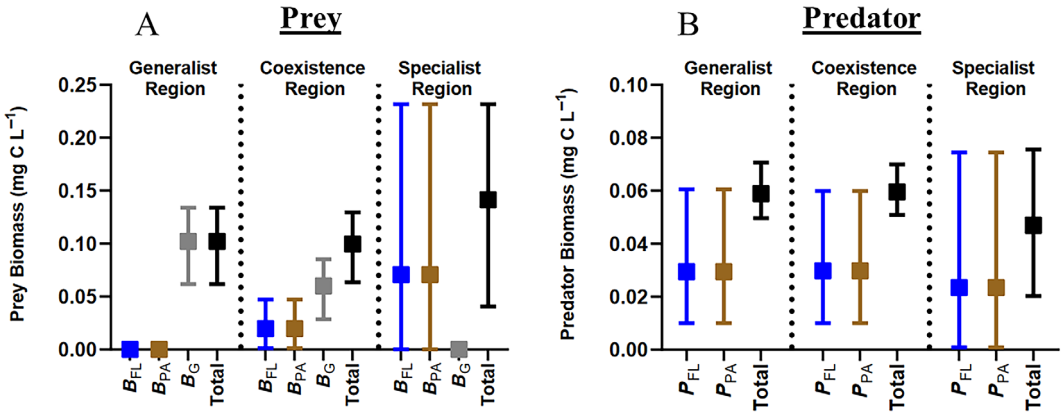

Fig. 6. Comparison of minimum, maximum, and average values of prey (**A**) and predator (**B**) biomass among generalist ($c = 0.02$), coexistence ($c = 0.2$) and specialist region ($c = 0.5$) with $S_{max} = 1$, $V = 0.7$. For average total prey biomass, the time average of calculated total biomass was taken.

Energy transfer to higher trophic levels

Comparing minimum, maximum, and average values for the different system states for $S_{max} = 1$ (Fig. 6), we observe that in the presence of B_G (generalist region and coexistence region) oscillations have a lower amplitude, and population minima are bound away from zero. Although in the specialist region, predator and prey undergo extreme cycles with long periods of population values near zero (Fig. 6, compare also Fig. 3E,I). The two specialist prey species gain the highest average biomass in the absence of the generalist (Fig. 6A). In contrast, the predator populations reach higher average biomasses in the presence of the generalist compared to only specialist prey species (Fig. 6B).

Discussion

Our study on a simplified bacterial model system reveals that the ability to adapt habitat choice in response to predation pressure and interspecific competition strongly influences community dynamics and composition. Specifically, our analysis shows that the parameter range for which the adaptive generalist can successfully establish is increasing with nutrient availability, making this strategy more successful in nutrient-rich environments. For low associated costs and a high speed of adaptation, the generalist can even out-compete the specialist competitors while sustaining both predator populations. However, associated energetic costs can only to a certain extent be compensated by a higher speed of adaptation, beyond which the generalist is always outcompeted by the specialists.

In our system, coexistence between generalist and specialist bacteria is only possible as part of an oscillatory attractor. This reflects the fact that under stable equilibrium conditions, the generalist, due to the associated energetic costs for being flexible, would always be out-competed as inferior resource competitor. This is consistent with other theoretical studies showing that asynchronous cycle dynamics are a prerequisite for coexistence between two specialists (fixed traits) and one generalist (flexible trait) consumer if limited by only two resources (Abrams 2006) or if competing for one resource in presence of a shared consumer (Yamamichi et al. 2011). Although coexistence is also possible under higher nutrient availability, where the system exhibits irregular oscillatory dynamics (Gaedke and Klauschies 2017), we restricted our analysis to the range of regular oscillatory dynamics to enable a mechanistic understanding of system dynamics dependent on increasing energetic costs and speed of adaptation. The investigated parameter range with respect to associated costs and speed of adaptation covers a broad range of biologically possible scenarios, where different species would be located at different positions on the parameter space. The results show that, especially if associated costs are low, the investigated behavioral defense mechanism enables coexistence of a habitat generalist with habitat specialist bacterial prey. This is related to the ability of the generalist to shift its biomass from one compartment to the alternative compartment, enabling to quickly reach higher biomass in the more favorable habitat compared to the specialist prey which has to increase from low numbers. Along the cycle this gives B_G an initial advantage in the resource competition before specialist prey and predator reach higher biomass levels. Furthermore, we observe a strong stabilizing influence of the adaptive generalist species on overall community dynamics, bounding cycle minima away from zero and leading to strongly reduced cycle amplitudes of protists, potentially allowing for a more regular and increased energy flow up to higher trophic levels compared to the specialist only case. The ability to shift the habitat, dependent on the speed of adaptation, enables the generalist to increase soon after the decrease of a predator which reduces the cycle amplitudes in comparison to the specialist only case and buffer the minima of predator biomass away from zero (*see* Supporting Information S8; Fig. 5).

A main difference to many existing studies on inducible defense is that, in our case, the ability to escape high

predation pressure in one habitat, makes the prey vulnerable to predation in the alternative habitat, also called incompatible defense (Ellner and Becks 2011; van Velzen et al. 2018). Hence, in such a system escape dynamics can only be temporarily effective, making it prone to oscillatory dynamics. Although our findings on the stabilizing influence of an inducible defense mechanism is in line with previous studies (Ives and Dobson 1987; Cortez 2011; Klauschies et al. 2016), the study by van Velzen et al. (2018) on an incompatible defense mechanism in a one-generalist prey-two-predator system, similar to our generalist only case, found the possibility of complete synchronization of the two generalist subpopulations for high exchange rates between phenotypes, leading to a destabilizing effect. These contrasting results are probably due to different implementations and therefore assumptions on the involved inducible defense mechanism. Although we use a fitness gradient approach with a dynamic trait parameter describing the change in the population mean trait value, van Velzen et al. (2018) explicitly consider two subpopulations (distinct phenotypes) with a fixed or adaptive exchange rate between them. Hence, in our case, a change in the (adaptive) trait immediately leads to a corresponding change in the distribution of the generalist population between the two habitats. In contrast, in the implementation of van Velzen et al. (2018) the distribution of the generalist population responds with a delay to a change in the exchange rate (biomass flow between the subpopulations). This further highlights the critical role of the implementation of inducible defense for system dynamics (Yamamichi et al. 2019*a*), which should be carefully chosen with respect to the involved mechanism. The implementation by van Velzen et al. (2018) can be considered to reflect mechanisms that involve morphological adaptations, creating a greater time lag when shifting between different subpopulations defined by different morpho-states, while our model implementation reflects a rapid behavioral escape response (see Supporting Information S9 for further details).

Furthermore, with regard to the implementation of the behavioral response, we assumed that the ability to adapt comes with increased maintenance costs, due to additional energy needed for the corresponding sensory and regulatory machinery (DeWitt et al. 1998), which was implemented by a respective decrease in the generalist growth rate. In principle, one could also imagine scenarios where the ability to adapt affects the half saturation constant or the overall mortality rate. Investigations of these additional scenarios show that the parameter that is influenced by additional costs has an effect on the range of coexistence, while the coexistence mechanism and associated community dynamics investigated in this study remain qualitatively the same (Supporting Information S7).

In our coupled system, we observe strong differences in the lags between specialist and generalist prey and their respective predators ranging from shorter than quarter-period lag to values close to one indicating reversed cycle dynamics (i.e., prey peak following the predator peak) (Cortez and Weitz 2014). In simple one predator-one prey systems, non-adaptive predator–prey cycles typically exhibit a quarter-period lag (Rosenzweig and MacArthur 1963; Bulmer 1975), while antiphase cycles are indicative for rapid evolution (Yoshida et al. 2003; Jones and Ellner 2007; Becks et al. 2012) as well as inducible defense mechanisms (Mougi 2012*a*,*b*; Yamamichi et al. 2019*a*) at the prey level. In our study system, antiphase cycles are only observed for total predator–prey dynamics, with lag values specifically matching 0.5 for the specialist only case. As described in the result section, this is related to the fact that our specialist predator–prey food web can also be interpreted as a coevolution model with clonal reproduction under a matching allele interaction (i.e., a predator clone can only consume the matching prey clone) (e.g., Grosberg and Hart 2000). Co-evolution along the bidirectional vulnerability axis is then represented by changes in the relative abundance of the two clones (species) in the total prey and predator population. Correspondingly, the specialist and the generalist only case can be seen as extreme cases of discrete vs. continuous trait adaptations at the prey level along a bidirectional vulnerability axis (Mougi 2012*a*; Yamamichi et al. 2019*b*) and illustrate dynamic consequences of genotype sorting vs. behavioral response mechanisms.

Looking at the single predator–prey lags, for the specialist only case each predator–prey pair follows the classic quarter-period lag, while for the generalist only case the predator–prey lags are significantly larger than the classic quarter-period lag and even longer than the expected half-period lag, if considering the shorter cycle length of the generalist population. In the range of coexistence, we observe two distinct patterns with time lags being similar to the generalist only case for low associated costs, where the generalist dominates the cycle dynamics, but generalist predator–prey lags increasing steeply once the specialist prey species start to dominate the cycle dynamics with increasing associated costs. This observation is due to the decreasing time window for the generalist species, determined by low competition and predation in one habitat, with increasing costs due to the increasing dominance of the specialist prey along the cycle, which strongly limits the biomass accumulation of the generalist population. In contrast, total prey and effective prey to predator lags initially show a steep decrease with increasing costs within the coexistence area, but settle on values matching the predator–prey lags of the specialist only case once the specialists start dominating the cycle dynamics. Overall cycle dynamics are speeded up in presence of the generalist compared to the specialist only case, reflecting differences between rapid behavioral responses vs. the slower response mechanism via clonal sorting.

Our model system can also be related to meta-community theory, reflecting a situation of two habitats connected by a moving prey. Similar investigations on meta-communities support our findings on the stabilizing influence of rapid prey

movement towards the most rewarding patch (Abrams 2000; Mougi 2019), being defined by inter-specific density dependent dispersal rates (Hauzy et al. 2010). This is an interesting aspect of the investigated model system and further extensions of the existing model to a spatially explicit approach might lead to more detailed insights on the influence of particle concentration on the bacterial community dynamics in aquatic environments with potential consequences for energy transport up to higher trophic levels.

This study used a strongly reduced conceptual representation of a natural aquatic microbial system to focus on the effect of adaptive vs. fixed habitat choice of free-living and particle-attached bacterial prey. Some of the simplifying assumptions shall be discussed in the following section. A central assumption in our model is the shared nutrient pool for all bacteria, which precludes the investigation of effects of particles that themselves are a source of carbon/nutrients. Although this assumption enabled to focus on the effect of flexible habitat choice, avoiding the rather complex remineralization processes of dissolved organic material and its effects on competition between specialist and generalist bacteria, it limits the implications of the model system to be best comparable to non-organic particles like microplastics, where particle-attached bacteria rely on carbon sources/nutrients from the surrounding water. Even with this limitation, the model points to important implications for bacterial community dynamics and energy transport via the microbial loop given the global increase in plastic litter, which has become the most abundant form of marine debris (Derraik 2002; Andrady 2011; Cole et al. 2011) and is common to all environments: oceans (Law 2017), freshwaters (Eerkes-Medrano et al. 2015), polar environments (Obbard et al. 2014) and even pristine mountain lakes (Free et al. 2014). Several studies show a high colonization rate of bacteria and protists on microplastics and the development of complex biofilm structures with bacteria, fungi, phytoplankton, protists, and so on (Kettner et al. 2019; Amaral-Zettler et al. 2020).

Another simplifying model assumption is that the particle compartment is only indirectly implemented through habitat-specific predators. Therefore, in its current form, the model does not capture the relative sizes of water vs. particle compartment. In nature the particle compartment will offer less surface area for colonization compared to the available volume of ambient water. This will restrict the maximum bacterial biomass that can accumulate on inorganic as well as organic particles. Relative compartment size will influence cycle amplitudes and likely reduce the range of coexistence for the generalist, if there is a mismatch between compartments with respect to possible maximum biomass that can be reached. A further simplifying assumption is the parameter choice with identical physiological parameters for all preys and predators, leading to a case of large synchrony between compartments. While this is not realistic, we still claim that our model results adequately capture the main dynamic features of the investigated model system. This is supported by additional analysis assuming different conversion efficiencies between preys and predators (*see* Supporting Information S1) and different growth/consumption rates between compartments (*see* Supporting Information S2), which lead to the same qualitative results as in the main study.

Especially for the case of inorganic particles, results from our model system can be indicative for consequences of the presence of different bacterial lifestyles for energy flow through the microbial loop to higher trophic levels in pelagic systems. Trait adaptations that influence species interactions potentially drive changes in community dynamics that, in turn, affect ecosystem functions (Matthews et al. 2011). Results from our study system suggest that the presence of generalist bacterial prey leads to higher average predator biomass compared to the presence of only specialist prey, enabling also increased energy flow to higher trophic levels. Furthermore, predator minima are more bound away from zero, leading to increased stability in the presence of generalist prey. Our results indicate that, especially in nutrient-rich environments, generalists could play an important role in the contribution of the microbial loop to energy flow in pelagic systems (Cho and Azam 1988; Pomeroy et al. 1991; Sherr and Sherr 2002). But also in oligotrophic environments, the presence of the generalist bacterial prey species is predicted to have a positive effect on system stability and enhance the transfer of organic matter through the food web.

Our modeling approach is an attempt to gain insight on consequences of adaptive dynamics at the base of the aquatic food web with respect to niche differentiation in pelagic environments. The specialization of microbes to water or particles (Grossart 2010) does not only define microbial lifestyle, but also influences processes and dynamics in pelagic environments, for example, organic matter turnover, which is important for nutrient losses to the sediments. Adaptive dynamics related to bacterial lifestyle could potentially affect community dynamics, but are not trivial to assess in nature. Therefore, experiments and modeling simulations are very useful to better understand these behavioral processes and its ecological consequences. Such an understanding is of high importance in light of observed and projected changes in precipitation patterns and the occurrence of extreme weather events like heavy rainfalls, floods or strong winds due to climate change, which will potentially increase the input of suspended particles (Perga et al. 2018). This in combination with the global thread of microplastics (Cole et al. 2011; Free et al. 2014; Eerkes-Medrano et al. 2015) necessitates studies to better understand the impact of inorganic particles on (microbial) food web interactions and predict consequences for energy flow in aquatic systems.

Data Availability Statement

No data were used.

References

Abrams, P. A., H. Matsuda, and Y. Harada. 1993. Evolutionarily unstable fitness maxima and stable fitness minima of continuous traits. Evol. Ecol. **7**: 465–487. doi:10.1007/BF01237642

Abrams, P. A., and H. Matsuda. 1997. Prey adaptation as a cause of predator–prey cycles. Evolution **51**: 1742–1750. doi:10.1111/j.1558-5646.1997.tb05098.x

Abrams, P. A. 2000. The impact of habitat selection on the spatial heterogeneity of resources in varying environments. Ecology **81**: 2902–2913.

Abrams, P. A. 2006. The prerequisites for and likelihood of generalist-specialist coexistence. Am. Nat. **167**: 329–342. doi:10.1086/499382

Amaral-Zettler, L. A., E. R. Zettler, and T. J. Mincer. 2020. Ecology of plastisphere. Nat. Rev. Microbiol. **18**: 139–151. doi:10.1038/s41579-019-0308-0

Andrady, A. M. 2011. Microplastics in the marine environment. Mar. Pollut. Bull. **62**: 1596–1605. doi:10.1016/j.marpolbul.2011.05.030

Azam, F., T. Fenchel, J. G. Field, J. S. Gray, L. A. Meyer-Reil, and J. Thingstad. 1983. The ecological role of water-column microbes in the sea. Mar. Ecol. Prog. Ser. **10**: 257–263.

Becks, L., S. P. Ellner, L. E. Jones, and N. G. Hairston. 2012. The functional genomics of an eco-evolutionary feedback loop: Linking gene expression, trait evolution, and community dynamics. Ecol. Lett. **15**: 492–501. doi:10.1111/j.1461-0248.2012.01763.x

Boenigk, J., and H. Arndt. 2002. Bacterivory by heterotrophic flagellates: Community structure and feeding strategies. Antonie Van Leeuwenhoek **81**: 465–480. doi:10.1023/a:1020509305868

Brown, P. N., G. D. Byrne, and A. C. Hindmarsh. 1989. VODE: A variable-coefficient ODE solver. SIAM J. Sci. Statist. Comp. **10**: 1038–1051.

Bulmer, M. G. 1975. Phase relations in the ten-year cycle. J. Anim. Ecol. **44**: 609–621.

Cho, B. C., and F. Azam. 1988. Major role of bacteria in biogeochemical fluxes in the ocean's interior. Nature **332**: 441–443.

Cole, M., P. Lindeque, C. Halsband, and T. S. Galloway. 2011. Microplastics as contaminants in the marine environment: A review. Mar. Pollut. Bull. **62**: 2588–2597. doi:10.1016/j.marpolbul.2011.09.025

Corno, G., I. Salka, K. Polhmann, A. R. Hall, and H. P. Grossart. 2015. Interspecific interactions drive chitin and cellulose degradation by aquatic microorganisms. Aquat. Microb. Ecol. **76**: 27–37. doi:10.3354/ame01765

Cortez, M. H. 2011. Comparing the qualitatively different effects rapidly evolving and rapidly induced defences have on predator–prey interactions. Ecol. Lett. **14**: 202–209. doi:10.1111/j.1461-0248.2010.01572.x

Cortez, M. H., and J. S. Weitz. 2014. Coevolution can reverse predator-prey cycles. Proc. Natl. Acad. Sci. USA **111**: 7486–7491. doi:10.1073/pnas.1317693111

Derraik, J. G. B. 2002. The pollution of the marine environment by plastic debris: A review. Mar. Pollut. Bull. **44**: 842–852. doi:10.1016/S0025-326X(02)00220-5

DeWitt, T. J., A. Sih, and D. S. Wilson. 1998. Costs and limits of phenotypic plasticity. Trends Ecol. Evol. **13**: 77–81. doi:10.1016/s0169-5347(97)01274-3

Eerkes-Medrano, D., R. C. Thompson, and D. C. Aldridge. 2015. Microplastics in freshwater systems: A review of the emerging threats, identification of knowledge gaps and prioritisation of research needs. Water Res. **75**: 63–82. doi:10.1016/j.watres.2015.02.012

Ellner, S. P., and L. Becks. 2011. Rapid prey evolution and the dynamics of two predator food-webs. Theor. Ecol. **4**: 133–152. doi:10.1007/s12080-010-0096-7

Fenchel, T. 1984. Suspended marine bacteria as a food source, p. 301–316. *In* M. J. R. Fasham [ed.], Flows of energy and materials in marine ecosystems. Plenum Press.

Free, C. M., O. P. Jensen, S. A. Mason, M. Eriksen, N. J. Williamson, and B. Boldgiv. 2014. High-levels of microplastic pollution in a large, remote, mountain lake. Mar. Pollut. Bull. **85**: 156–163. doi:10.1016/j.marpolbul.2014.06.001

Gaedke, U., and T. Klauschies. 2017. Integrating food-web and trait-based ecology to investigate biomass-trait-feedbacks, p. 107–120. *In* J. C. Moore, P. De Ruiter, K. McCann, and V. Wolters [eds.], Adaptive food webs: Stability and transitions of real and model ecosystems. Cambridge Univ. Press.

Garcia, S. L., I. Salka, H. P. Grossart, and F. Warnecke. 2013. Depth-discrete profiles of bacterial communities reveal pronounced spatio-temporal dynamics related to lake stratification. Environ. Microbiol. Rep. **5**: 549–555. doi:10.1111/1758-2229.12044

Garcia-Chaves, M. C., M. T. Cottrell, D. L. Kirchman, A. M. Derry, M. J. Bogard, and P. A. del Giorgio. 2015. Major contribution of both zooplankton and protists to the top-down regulation of freshwater aerobic anoxygenic phototrophic bacteria. Aquat. Microb. Ecol. **76**: 71–83. doi:10.3354/ame01770

Grosberg, R., and M. Hart. 2000. Mate selection and the evolution of highly polymorphic self/nonself recognition genes. Science **289**: 2111–2114. doi:10.1126/SCIENCE.289.5487.2111

Grossart, H. P. 2010. Ecological consequences of bacterioplankton lifestyles: Changes in concepts are needed. Environ. Microbiol. Rep. **2**: 706–714. doi:10.1111/j.1758-2229.2010.00179.x

Hahn, M. W., E. R. Moore, and M. G. Höfle. 2000. Role of microcolony formation in the protistan grazing defence of the aquatic bacterium *Pseudomonas* sp. MWH1. Microb. Ecol. **39**: 175–185. doi:10.1007/s002480000026

Hauzy, C., M. Gauduchon, F. D. Hulot, and M. Loreau. 2010. Density-dependent dispersal and relative dispersal affect the stability of predator–prey metacommunities. J. Theor. Biol. **266**: 458–469. doi:10.1016/j.jtbi.2010.07.008

Ives, A. R., and A. P. Dobson. 1987. Antipredator behavior and the population dynamics of simple predator-prey systems. Am. Nat. **130**: 431–447. doi:10.1086/284719

Jones, L. E., and S. P. Ellner. 2007. Effects of rapid prey evolution on predator–prey cycles. J. Math. Biol. **55**: 541–573.

Kassen, R. 2002. The experimental evolution of specialists, generalists, and the maintenance of diversity. J. Evol. Biol. **15**: 173–190. doi:10.1046/j.1420-9101.2002.00377.x

Kats, L. D., and L. M. Dill. 1998. The scent of death: Chemosensory assessment of predation risk by prey animals. Ecosci. **5**: 361–394. doi:10.1080/11956860.1998.11682468

Kettner, M. T., S. Oberbeckmann, M. Labrenz, and H. P. Grossart. 2019. The eukaryotic life on microplastics in brackish ecosystems. Front. Microbiol. **10**: 538. doi:10.3389/fmicb.2019.00538

Kiørboe, T., K. Tang, H. P. Grossart, and H. Ploug. 2003. Dynamics of microbial communities on marine snow aggregates: Colonization, growth, detachment, and grazing mortality of attached bacteria. Appl. Environ. Microbiol. **69**: 3036–3047. doi:10.1128/AEM.69.6.3036-3047.2003

Kiørboe, T., H. P. Grossart, H. Ploug, K. Tang, and B. Auer. 2004. Particle-associated flagellates: Swimming patterns, colonization rates, and grazing on attached bacteria. Aquat. Microb. Ecol. **35**: 141–152. doi:10.3354/ame035141

Klauschies, T., D. A. Vasseur, and U. Gaedke. 2016. Trait adaptation promotes species coexistence in diverse predator and prey communities. Ecol. Evol. **6**: 4141–4159. doi:10.1002/ece3.2172

Law, K. L. 2017. Plastics in the marine environment. Ann. Rev. Mar. Sci. **9**: 205–229. doi:10.1146/annurev-marine-010816-060409

Matthews, B., and others. 2011. Toward an integration of evolutionary biology and ecosystem science. Ecol. Lett. **14**: 690–701. doi:10.1111/j.1461-0248.2011.01627.x

Mougi, A. 2012*a*. Predator-prey coevolution driven by size selective predation can cause anti-synchronized and cryptic population dynamics. Theor. Popul. Biol. **81**: 113–118. doi:10.1016/j.tpb.2011.12.005

Mougi, A. 2012*b*. Unusual predator-prey dynamics under reciprocal phenotypic plasticity. J. Theor. Biol. **305**: 96–102. doi:10.1016/j.jtbi.2012.04.012

Mougi, A. 2019. Adaptive migration promotes food web persistence. Sci. Rep. **9**: 1–5.

Obbard, R. W., S. Sadri, Y. Q. Wong, A. A. Khitun, I. Baker, and R. C. Thompson. 2014. Global warming releases microplastic legacy frozen in Arctic Sea ice. Earth Futur. **2**: 315–320. doi:10.1002/2014EF000240

Parry, J. D. 2004. Protozoan grazing of freshwater biofilms. Adv. Appl. Microbiol. **54**: 167–196. doi:10.1016/s0065-2164(04)54007-8

Perga, M. E., R. Bruel, L. Rodriguez, Y. Guénand, and D. Bouffard. 2018. Storm impacts on alpine lakes: Antecedent weather conditions matter more than the event intensity. Glob. Chang. Biol. **24**: 5004–5016. doi:10.1111/gcb.14384

Pomeroy, L. R., W. J. Wiebe, D. Deibel, R. J. Thompson, G. T. Rowe, and J. D. Pakulsky. 1991. Bacterial responses to temperature and substrate concentration during the Newfoundland spring bloom. Mar. Ecol. Prog. Ser. **75**: 143–159.

Rosenzweig, M. L., and R. H. MacArthur. 1963. Graphical representation and stability conditions of predator–prey interactions. Am. Nat. **97**: 209–223.

Seiler, C., E. van Velzen, T. R. Neu, U. Gaedke, T. U. Berendonk, and M. Weitere. 2017. Grazing resistance of bacterial biofilms: A matter of predators' feeding trait. FEMS Microbiol. Ecol. **93**: 1–9. doi:10.1093/femsec/fix112

Sherr, E. B., and B. F. Sherr. 1988. Role of microbes in pelagic food webs: A revised concept. Limnol. Oceanogr. Comment. **33**: 1225–1227.

Sherr, E. B., and B. F. Sherr. 2002. Significance of predation by protists in aquatic microbial food webs. Int. J. Gen. Mol. Microbiol. **81**: 293–308. doi:10.1023/A:1020591307260

Simon, M., H. P. Grossart, B. Schweitzer, and H. Ploug. 2002. Microbial ecology of organic aggregates in aquatic ecosystems. Review. Aquat. Microb. Ecol. **25**: 175–211. doi:10.3354/ame028175

van Velzen, E., and U. Gaedke. 2017. Disentangling eco-evolutionary dynamics of predator-prey coevolution: The case of antiphase cycles. Sci. Rep. **7**: 17125. doi:10.1038/s41598-017-17019-4

van Velzen, E., T. Thieser, T. Berendonk, M. Weitere, and U. Gaedke. 2018. Inducible defence destabilizes predator–prey dynamics: The importance of multiple predators. Oikos **127**: 1551–1562. doi:10.1111/oik-04868

Verschoor, A. M., M. Vos, and I. van der Stap. 2004. Inducible defences prevent strong population fluctuations in bi- and tritrophic food chains. Ecol. Lett. **7**: 1143–1148. doi:10.1111/j.1461-0248.2004.00675

Vos, M., B. W. Kooi, D. L. DeAngelis, and W. M. Mooij. 2004. Inducible defences and the paradox of enrichment. Oikos **105**: 471–480. doi:10.1111/j.0030-1299.2004.12930.x

Williams, P. J., and leB. 1981. Microbial contribution to overall marine plankton metabolism: Direct measurements of respiration. Oceanol. Acta **4**: 359–364.

Yamamichi, M., T. Yoshida, and A. Sasaki. 2011. Comparing the effects of rapid evolution and phenotypic plasticity on predator–prey dynamics. Am. Nat. **178**: 287–304. doi:10.1086/661241

Yamamichi, M., T. Klauschies, B. E. Miner, and E. van Velzen. 2019*a*. Modelling inducible defences in predator–prey interactions: Assumptions and dynamical consequences of three distinct approaches. Ecol. Lett. **22**: 390–404. doi:10.1111/ele.13183

Yamamichi, M., K. Lyberger, and S. Patel. 2019*b*. Antagonistic coevolution between multiple quantitative traits: Matching dynamics can arise from difference interactions. Popul. Ecol. **61**: 362–370. doi:10.1002/1438-390X-12022

Yoshida, T., L. E. Jones, S. P. Ellner, G. F. Fussmann, and N. G. Hairston. 2003. Rapid evolution drives ecological dynamics in a predator-prey system. Nature **424**: 303–306. doi:10.1038/nature01767

Acknowledgments

The authors thank Jason Woodhouse and two anonymous reviewers for helpful suggestions to improve this manuscript. This project was funded by the German Research Foundation (DFG) Priority Program 1704: DynaTrait (GR 1540/25-1+2, WO 2273/1-1). The work was partly funded by the German Federal Ministry of Education and Research BMBF within the Collaborative Project "Bridging in Biodiversity Science - BIBS" (funding number 01LC1501). All responsibility for the content of this publication is assumed by the author. Open Access funding enabled and organized by Projekt DEAL.

Conflict of Interest

None declared.

Submitted 21 May 2020
Revised 08 December 2020
Accepted 27 March 2022

Associate editor: Takehito Yoshida